Structured networks support sparse traveling waves in rodent somatosensory cortex

Samat Moldakarimov[a,b], Maxim Bazhenov[a,c], Daniel E. Feldman[d], and Terrence J. Sejnowski[a,b,e,1]

[a]Howard Hughes Medical Institute, The Salk Institute for Biological Studies, La Jolla, CA 92037; [b]The Institute for Neural Computation, University of California, San Diego, La Jolla, CA 92093; [c]Department of Medicine, University of California, San Diego, La Jolla, CA 92093; [d]Department of Molecular and Cell Biology, University of California, Berkeley, CA 94720; and [e]Division of Biological Sciences, University of California, San Diego, La Jolla, CA 92093

Contributed by Terrence J. Sejnowski, March 27, 2018 (sent for review June 12, 2017; reviewed by Idan Segev and Karel Svoboda)

Neurons responding to different whiskers are spatially intermixed in the superficial layer 2/3 (L2/3) of the rodent barrel cortex, where a single whisker deflection activates a sparse, distributed neuronal population that spans multiple cortical columns. How the superficial layer of the rodent barrel cortex is organized to support such distributed sensory representations is not clear. In a computer model, we tested the hypothesis that sensory representations in L2/3 of the rodent barrel cortex are formed by activity propagation horizontally within L2/3 from a site of initial activation. The model explained the observed properties of L2/3 neurons, including the low average response probability in the majority of responding L2/3 neurons, and the existence of a small subset of reliably responding L2/3 neurons. Sparsely propagating traveling waves similar to those observed in L2/3 of the rodent barrel cortex occurred in the model only when a subnetwork of strongly connected neurons was immersed in a much larger network of weakly connected neurons.

traveling wave | sensory cortex | cortical organization | small-world network | space–time population code

Linking cortical functions to the underlying cortical organization is one of the most important problems in neuroscience. Cortical layer 2/3 (L2/3) serves as an important output layer during the hierarchical processing of sensory information within the sensory cortices, and thus, understanding L2/3 organization is critical for understanding computation in canonical cortical circuits (1).

In contrast to sensory cortices of larger animals (carnivores and primates), where neurons in the superficial cortical layer 2/3 (L2/3) tuned for different sensory stimuli are spatially organized in cortical maps (2), L2/3 in the rodent sensory cortices lacks crystalline maps with strong local tuning heterogeneity. Instead, calcium imaging studies in rats and mice show that in L2/3 of primary sensory cortices (visual, auditory, and somatosensory) neurons tuned for different stimuli are spatially intermixed and result in a salt-and-pepper organization (3–6). In the somatosensory (barrel) cortex of the rodents, this heterogeneity was observed by stimulating a single whisker, which evoked spikes in distributed neuronal population that spanned multiple whisker-related anatomical columns (7–11) (Fig. 1 *A* and *B*).

The neural response properties in L2/3 of the rodent barrel cortex also differ significantly compared with neural responses in sensory cortices of larger animals. In larger animals, L2/3 neurons respond reliably to sensory stimuli (2), whereas in the rodent barrel cortex, deflection of the principal (preferred) whisker evokes low-probability spiking responses in the majority of responding L2/3 neurons, yielding mean overall firing rate of <0.1 Hz (12–16). However, a small fraction of L2/3 neurons (~10%) have higher whisker-evoked response probability, resulting in a skewed distribution of response probabilities across L2/3 neurons (17, 18).

Here we explain how the superficial layer 2/3 of the rodent barrel cortex could be organized to account for these observations.

Hypothesis

In a computer model of L2/3 of the rodent barrel cortex, we attempt to explain cortical organization and neural response properties in L2/3 by combining two observations: (*i*) propagation of activity in the rodent barrel cortex in response to whisker stimulation (8–10) and (*ii*) lognormal distributions of synaptic weights observed in many cortical areas (19).

Stimulus-evoked propagation of activity has been observed in the rodent barrel cortex in response to whisker stimulation using voltage-sensitive dyes (Fig. 1*D*) (8, 9), but the cortical circuits that support the activity propagation have not been previously explored. There is evidence that the activity propagation in the rodent barrel cortex could be supported by strong horizontal connections (20) [although intracolumnar interactions across layers may also contribute to the activity propagation (21)]. We will show that the observed salt-and-pepper tuning, low average responsiveness, and the existence of a population of more reliably responding L2/3 neurons in the rodent barrel cortex can all be explained by activity propagation within L2/3.

There is converging evidence for nonrandom organization of the synaptic connections in the brain networks (22). In contrast to random networks, where synaptic weights follow a Poisson distribution (19), in brain networks the distribution of synaptic weights follows a lognormal distribution, indicating that most of the connections are short and weak, but there exist a few stronger and longer synaptic connections. In the rodent visual and somatosensory cortex, neurons with stronger synapses are preferentially connected with each other (23–25). Thus, effectively cortical network structure in the rodent barrel cortex could

Significance

The deflection of a single whisker activates neurons in the corresponding barrel of rodent somatosensory cortex, which is followed by a traveling wave of activity across the upper layer 2/3 (L2/3) of barrel cortex. There are many ways to generate traveling waves, but the model that we propose is the only one that is constrained by the data from the barrel cortex. We also explain the importance of traveling waves for encoding sensory stimuli in the barrel cortex and show how whisker stimulation induces horizontal propagation of activity within the barrel cortex with the observed sparse neural activity. Our theory contrasts the conventional theory of sensory processing, which assumes feedforward processing in hierarchically organized cortical networks.

Author contributions: S.M., M.B., D.E.F., and T.J.S. designed research; S.M. performed research; and S.M., M.B., D.E.F., and T.J.S. wrote the paper.

Reviewers: I.S., Hebrew University; and K.S., Howard Hughes Medical Institute.

The authors declare no conflict of interest.

[1]To whom correspondence should be addressed. Email: terry@salk.edu.

This article contains supporting information online at www.pnas.org/lookup/suppl/doi:10.1073/pnas.1710202115/-/DCSupplemental.

Published online April 30, 2018.

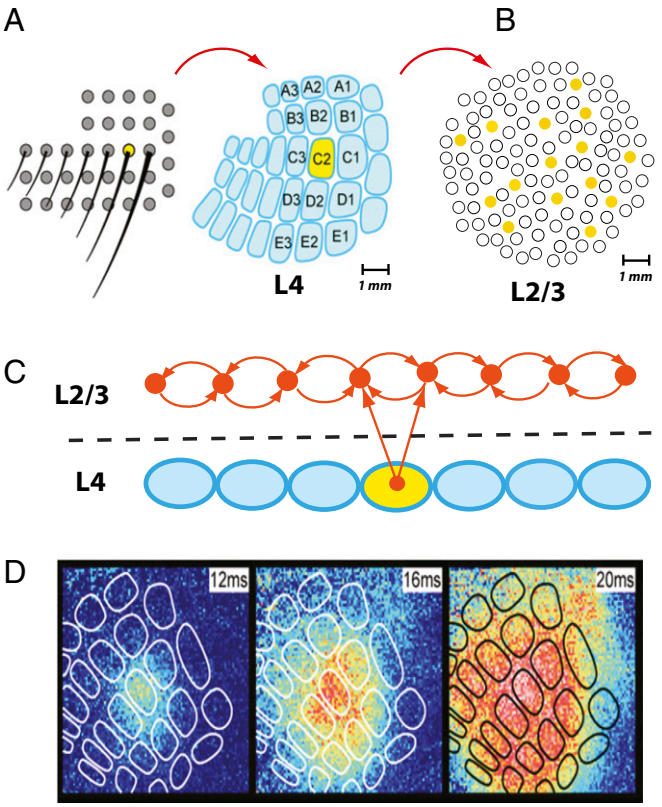

Fig. 1. Sensory representation in rodent somatosensory cortex. (*A*) Schematic illustration of the rodent whisker pads and the corresponding whisker pads in the input layer 4 of the rodent barrel cortex; reprinted with permission from ref. 9, permission conveyed through Copyright Clearance Center, Inc. (*B*) Illustrations of distributed sensory representation in layer L2/3. Stimulation of a whisker marked by yellow in *A* results in localized activity in the input layer 4 and distributed activity in the superficial layer 2/3. (*C*) A 2D neural network model of the superficial layer 2/3. The input from cortical layer 4 was implemented by injecting currents directly into L2/3 neurons. (*D*) Experimental demonstration of activity propagation in L2/3 of the rodent barrel cortex in response to whisker stimulation; reprinted with permission from ref. 9, permission conveyed through Copyright Clearance Center, Inc. The activity was assessed using voltage-sensitive dyes, which primarily reported subthreshold changes of the membrane voltages.

be viewed as a network in which a subset of strongly connected neurons immersed in a network of weakly connected neurons.

Model

To examine the consequences of this hypothesis we developed a neural network model that included essential features of the L2/3 circuits in barrel cortex (26–28). Although the model was an extreme simplification of S1 cortex anatomy, it highlighted important circuit mechanisms underlying cortical responses to sensory stimuli.

The model consisted of 10,000 excitatory and 2,500 inhibitory spiking neurons arranged in a 2D network. The excitatory neurons were modeled after pyramidal neurons (29), and the inhibitory neurons were modeled after fast-spiking PV interneurons (30–32).

In the rodent barrel cortex, 10% of L2/3 neurons respond with much higher probability than the rest of L2/3 neurons (17, 18). We assume that the experimentally observed L2/3 neurons respond with much higher probability than other responding L2/3 neurons because these neurons are preferentially connected with each other via stronger connections. Thus, in the model, we assume that 10% of the excitatory in L2/3 neurons connected via stronger connections than the rest of L2/3 neurons. These strongly connected neurons are immersed in a network of weakly connected neurons (Fig. 2*A*). These model assumptions resulted in a skewed distribution of synaptic weights (Fig. 2*B*), similar to the distributions of synaptic weights observed in many cortical areas (19).

Results

A Subnetwork of Strongly Connected Neurons Supports Activity Propagation in L2/3. We stimulated a small population of randomly selected neurons in the center of L2/3 network, which mimicked inputs from layer 4 neurons. We wanted to reproduce the observed propagation of activity in response to the deflection of a single whisker (Fig. 1*D*) (6–11). We assumed that 10% of excitatory L2/3 neurons were connected via stronger synapses, and these strong connections are critical to support the activity propagation within L2/3. However, it was not clear how many strong connections are needed in the network to support such activity propagation. Thus, the only parameter we varied in the model was the number of strong connections among randomly selected 10% of excitatory L2/3 neurons.

We increased the number of the strong connections until we observed propagation of spiking activity in the network (Figs. 2*C* and 3 *A* and *B*). This occurred in the model when we randomly connected 1,000 excitatory neurons with 500 strong connections. This result was theoretically predicted in a seminal paper on random networks (33), where it was shown that there is a critical number of connections among units of a random network, when a subnetwork of interconnected units reaches the size of the whole network. In theory, this condition emerges when the

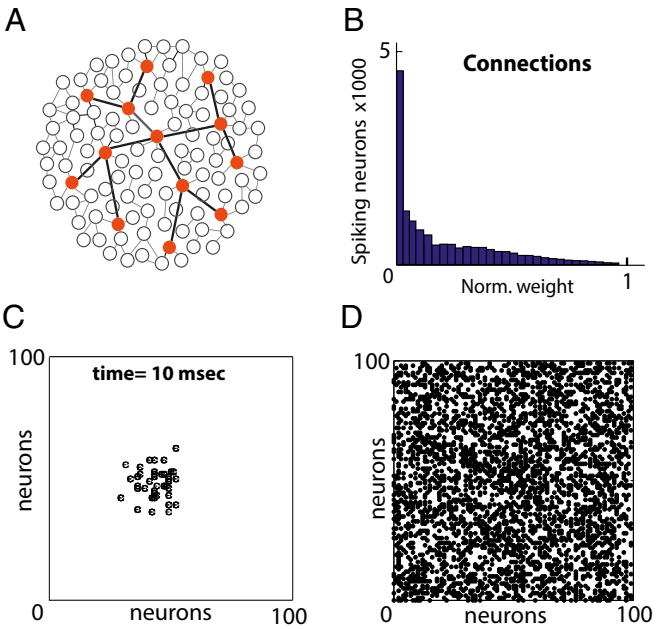

Fig. 2. Neural network model of the rodent barrel cortex. (*A*) A strongly connected subnetwork of L2/3 that constituted 10% of the excitatory neurons (red circles). (*B*) Distribution of synaptic strengths of the excitatory neurons. The majority of L2/3 neurons had weak short-range synapses, and only a few were connected via strong long-range synapses. This skewed the distribution of synaptic connections. (*C*) Model simulation. Stimulus-evoked activity failed to propagate through the network. One hundred stronger synapses were distributed among randomly selected 1,000 excitatory L2/3 neurons. (*D*) Model simulation. The same network as in *C* with a higher density of strong connections among the excitatory neurons. Stimulus-evoked activity propagated through the network, but the activity continued long after the stimulation was terminated. Nine hundred stronger synapses were distributed among randomly selected 1,000 excitatory L2/3 neurons.

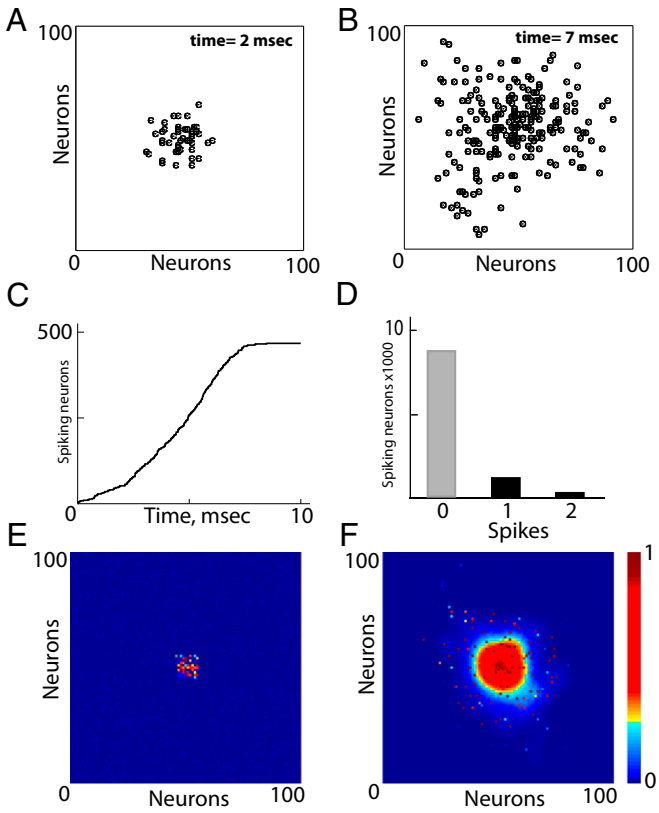

Fig. 3. Activity propagation in the neural network model. (*A* and *B*) Activity patterns at two time intervals in a network with 500 stronger synapses distributed among randomly selected 1,000 excitatory L2/3 neurons. In contrast to Fig. 2*D*, the propagated activity was sparser and terminated when the activity reached the boundaries of the network. (*C*) The total number of responding L2/3 neurons as a function of time. (*D*) Spike histogram of L2/3 neurons after a single stimulus presentation. (*E*) Membrane potentials of L2/3 neurons after 2 ms. A few L2/3 spiked at the center of the network. (*F*) Membrane potentials of L2/3 neurons after 5 ms. The wave of depolarization of the membrane voltage could be observed, but the majority of L2/3 neurons did not spike. The propagation of activity reflected the subthreshold membrane voltage.

number of connections is half of the number of units in the network (33). In our model, this happened when we randomly selected 1,000 neurons and connected them with 500 strong connections.

When we increased the number of the strong connections beyond this threshold, the evoked activity not only propagated through the network but was present in the network long after the activity reached the boundaries of the network (Fig. 2*D*). This result indicated that the strong connections also supported the sustained reverberating activity, when the density of the strong connections was too high. When the density of the strong connections was at the predicted threshold, the activity propagated in the network and terminated when the activity reached the boundaries of the network (Fig. 3 *A* and *B*).

Sparseness of Propagated Activity in L2/3 Network. The propagated activity in L2/3 was spatially sparse: although the propagated activity reached the boundaries of the network, most of L2/3 excitatory neurons did not spike in response to stimulation (Fig. 3*C*). Because the propagating activity in L2/3 did not cause spiking in every neuron at the wavefront, and the density of the strong connections determined the propagation of activity, it is likely that the activity traveled mostly over the strong connections.

The evoked activity in L2/3 was also temporally sparse: the responding L2/3 neurons only fired one or two spikes (Fig. 3*D*). This included both the neurons responding with higher probability and the low-probability responding neurons. The temporal sparseness of neural responses in L2/3 was due to the short stimulation of L2/3 neurons by L4 neurons (due to feedforward inhibition that followed feedforward excitation) and the short wavefront within L2/3. This modeling result is consistent with the previous observation that even the most reliably responding neurons in L2/3 of the rodent barrel cortex produce no more than a few spikes (34).

Propagation of Subthreshold Activity. We also reproduced the previously observed results obtained using voltage-sensitive dyes, which we suggest mainly reflect subthreshold activity (8, 9). In the model, although the propagated activity resulted in sparse spiking activity (Fig. 3 *A* and *B*), the subthreshold activity was dense (Fig. 3 *E* and *F*); in the majority of L2/3 neurons, membrane potentials increased as the activity propagated through the network. In the model, this was because the strongly responding neurons activated adjacent neurons via weak synapses, and most of the latter neurons could not reach the spiking threshold. Our observation is consistent with other experimental findings that show virtually all L2/3 pyramidal neurons exhibit reliable subthreshold postsynaptic potential in response to each whisker deflection, although few neurons spike on any individual trial (35).

It has been observed that L2/3 neurons that have the highest spike probability to whisker deflection are those with the highest E–I ratio (35). Thus, we suggest that inhibition can effectively control the spiking threshold in the excitatory neurons, which may result in sparse spiking activity under a wide range of stimuli.

Response Probabilities of L2/3 Neurons. In experimental results, deflection of the principal (preferred) whisker in rats evokes weak, low-probability spiking responses in the majority of responding L2/3 neurons, yielding mean overall firing rate of <0.1 Hz (12, 16). However, a small fraction of L2/3 neurons (~10%) have higher whisker-evoked response probability, resulting in a skewed distribution of response probabilities across L2/3 neurons (17, 18, 23–25, 34). These neural response properties in L2/3 also originate in the structure of the L2/3 network in our model.

In the model, we observed a skewed distribution of response probabilities in L2/3 neurons (Fig. 4*A*), which resulted from the skewed distribution of synaptic weights: the neurons with stronger synapses responded with a higher probability compared with other weakly connected L2/3 neurons. When we repeatedly presented the same stimulus, we observed different spatial patterns of spiking activity (Fig. 4*B*) because the low-probability spiking neurons participated in a small fraction of these activity patterns. Two patterns marked by black and gray dots represent two populations of L2/3 neurons responding with low probabilities on two separate trials. In these low-probability spiking L2/3 neurons, the neural activity in response to a stimulation was comparable with spontaneous activity (Fig. 4 *C* and *D*, blue vs. black bars), which resulted in probabilistic responses in these neurons.

In contrast, the highly active neurons responded to almost every application of the stimulus (Fig. 4*B*). The red dots represented L2/3 neurons that responded with a high probability to repeated presentation of the same stimulus.

Spike–Time Variation in L2/3 Neurons. We also observed differences in trial-to-trial variation of spike times between the low- and high-probability responding L2/3 neurons (Fig. 4 *D* and *F*). In the low-probability spiking neurons, we observed a higher spike–time

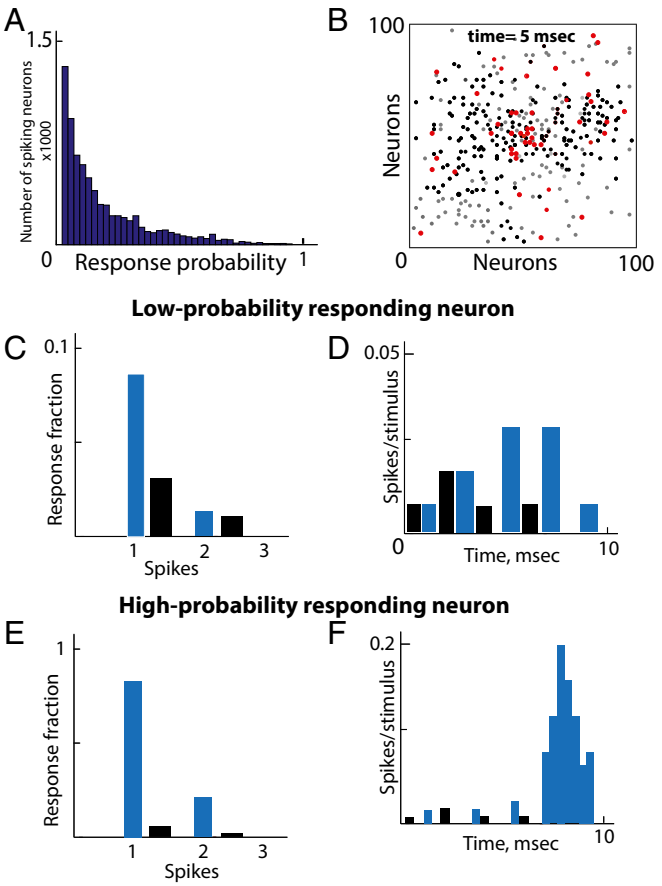

Fig. 4. Response properties of L2/3 neurons in the model. (*A*) The distribution of response probabilities in L2/3 neurons. (*B*) Activity patterns in the network of two presentations of a stimulus. The black and gray dots represent two populations of the low-probability responding L2/3 neurons showing that a different subset responded on the two trials. The red dots represent the high-probability responding neurons, which responded on most trials. (*C*) Spike histogram and (*D*) spike–time distribution in one of the low-probability responding L2/3 neurons. Neural activity in response to stimulation is shown by blue bars, and spontaneous activity is shown by black bars. (*E*) Spike histogram and (*F*) spike–time distribution in one of the high-probability responding neurons. Neural activity in response to stimulation is shown by blue bars, and spontaneous activity is shown by black bars.

variability (Fig. 4*D*) because spontaneous activity in the network made synaptic inputs noisy and significantly contributed to the observed trial-to-trial variation of spike times (Fig. 4*D*, blue vs. black bars). In the highly responsive neurons, spike times also varied for repeated presentation of a stimulus but less so than for the low-probabilistically responding neurons (Fig. 4*F*, blue vs. black bars). Stronger excitatory synaptic inputs reduced the effect of the input noise on spike initiation in these neurons, and a higher ratio of stimulus-evoked spikes to spontaneous spikes further reduced the observed spike–time variability. Thus, we predict that the strongly connected L2/3 neurons must show lower trial-to-trial variations of spike times than other probabilistically responding L2/3 neurons. It is consistent with finding in the rodent visual cortex, where strongly connected neurons spike more reliably in response to stimulation (25).

Discussion

The sensory representation and neural response properties in L2/3 of the rodent barrel cortex differ significantly compared with neural responses in sensory cortices of larger animals (2–7). In a computer model of L2/3 of the rodent barrel cortex, we explained cortical organization and neural response properties in L2/3 by combining two observations: (*i*) propagation of activity in the rodent barrel cortex in response to whisker stimulation (8, 9) and (*ii*) lognormal distributions of synaptic weights observed in many brain areas (19).

We showed in the model that stimulus-evoked activity propagation in the barrel cortex could be supported by intracolumnar and cross-columnar horizontal connections (20), but intracolumnar interactions across layers may also contribute to the activity propagation (21). Based on our simulations we predict that connections among strongly responding layer 2/3 excitatory neurons could be on average stronger and longer than in other weakly responding L2/3 neurons.

Our model exhibited a few previously observed neuronal properties in L2/3 in the rodent barrel cortex: the low response probability in the majority of L2/3 neurons and the existence of a small subset of the highly responsive L2/3 neurons. Our model predicts the significant differences in spike precision among the low- and high-probability responding L2/3 neurons. Taking into account that the strongly responding L2/3 neurons are sparsely distributed (23), we further predict that there might be a counterintuitive positive correlation between the strengths of connections and the distance between these strongly responding L2/3 neurons.

Despite the sparse pattern of spiking in the network of weakly connected neurons, there was a high degree of correlation in their subthreshold membrane potentials, which could modulate the effect of other inputs. This could be explored by stimulating two or more whiskers in temporal sequences and observing the effect of the first whisker deflection on the responses of neurons to the second whisker deflection. During behavior, interactions between multiple whisker deflections could be much more complex.

Neural Code. The distributed sensory encoding formed by traveling waves is neither a rate code, because each neuron fires only a few spikes sporadically, nor a spike timing code, because of the great variability of first spike latency in a majority of the neurons. In such a space–time code, information is distributed in both spatial patterns and temporal spike patterns. What computations can be done with sparsely interacting traveling waves? For inspiration, in a recent study of the dynamics of a silicone droplet bouncing on a vibrating oil bath, the droplet created a set of waves, like the waves in barrel cortex evoked by a whisker deflection (36). The entire history of the droplet's path can be predicted from the observed spatial pattern at a single point in time. In a similar fashion, a neural wave traveling over the barrel cortex could encode both stimulus position and its recent history in a distributed spatiotemporal pattern of activation. The availability of information about the recent past could be useful in processing dynamic sensory patterns, which presents difficulties for static feedforward processing.

Salt-and-Pepper Sensory Tuning. Our model was developed to address experimental data obtained by stimulating a single whisker, in which one stimulus-specific subnetwork within L2/3 could be activated (24). However, the model also suggests an explanation for the emergence of the salt-and-pepper somatotopy in L2/3 (6–10). There is evidence that independent subnetworks of functionally distinct neural populations may coexist within single cortical columns (3, 37). Thus, we predict that in the rodent sensory cortices the salt-and-pepper somatotopy could be formed by overlapping subnetworks formed by specific sets of strongly connected L2/3 neurons, where each subnetwork tuned for a specific whisker covers many columns within the barrel cortex. Interactions among distinct but overlapping subnetworks may explain the broader receptive fields in the high-probability responding neurons (38).

Network Architecture. Our main results do not depend on a particular architecture of the network; many other networks may support activity propagation that may result in sparse spiking activity. We discuss a few possible network architectures that may support such sparse spiking activity.

The small-world architecture of neural systems has been reported in many studies on large-scale anatomy of mammalian cortex (39–41), for anatomical/functional small-world within cortical layers (42), and even on the cellular level (43). In our model, we assumed that there are two classes of connections, which resemble a small-world network; however, we have not tested if our network fits the definition of a classical small-world network.

A scale-free architecture for the subnetwork of strongly connected neurons could also support traveling waves (44). The subnetwork developed following the scale-free algorithm would result in a tree-like network, which can support activity propagation initiated at the center of the network without reverberating waves.

In their seminal paper on random networks (33), Erdos and Reniy showed that there is a critical number of connections among units of a random network, when one cluster of interconnected units becomes much larger than other clusters, and this largest cluster covers the entire network. This condition is called percolation threshold. Erdos and Reniy predicted that this threshold emerges when the number of connections is a half of the number of units in the network. Note that this is highly sparse connectivity because each of these connected neurons has on average less than one strong connection.

Erdos–Reniy theory also suggests an explanation on why we did not observe sustained activity at the percolation threshold. The theory predicts that probability of finding closed loops of connections in a random network is low at the percolation threshold. This suggests that in the model the strongly connected neurons form effectively a tree-like structure; therefore, the activity can propagate in this network without reverberating waves of activity.

Random networks at the percolation threshold could form fractals (45, 46). A critical advantage of fractal networks is that the fractal networks can cover larger areas with fewer connections. Taking into account that L2/3 may consist of many overlapping subnetworks, fractal networks may satisfy the requirement of the economy of cortical wiring (47). In contrast to regular objects, fractals have fractional dimensionalities. In a regular network, the density of strongly connected neurons should increase linearly with the area of observation. In a fractal network, the density should have a scaling exponent (typically less than one) with the area of measurement. Assuming that the strongly connected neurons are the neurons with stronger connections, the nonlinear dependences shown in Fig. 5 may indicate that the subnetwork of strongly connected neurons is fractal. However, the data may also indicate that the density of the evoked activity is unevenly distributed and may be higher in the center of the network due to the direct stimulation.

To further explore the circuit organization in L2/3 and distinguish between different network architectures (random, fractal, scale free, and small-world) it may be fruitful to ask the following questions: How do these L2/3 networks develop? Is it a random process that takes place simultaneously in many locations as in Erdos–Reniy model? Does the network start in a particular location and gradually add connections as in the scale-free networks? Are there two types of connections, local and global, as in the small-world networks? These and other questions could be explored in future studies.

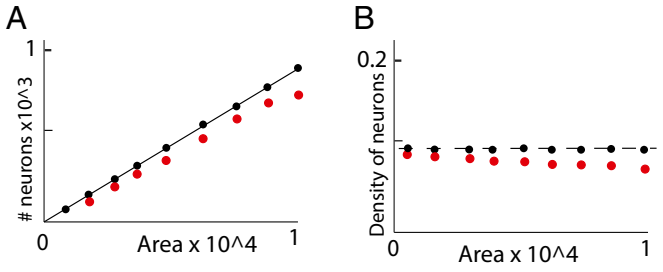

Fig. 5. Distribution of strongly responding neurons. (*A*) Number of strongly responding neurons as function of size of area over which the neurons were counted. Red circles are high-probability responding neurons, and black circles are low-probability responding neurons. (*B*) Density of neurons as function of size of area over which the neurons were counted.

Materials and Methods

See *SI Materials and Methods* for more details.

We developed a spiking neuron network model of L2/3 circuits of the rodent barrel cortex. Although the model is an extreme simplification of the rodent cortex anatomy, it highlights important circuit mechanisms underlying cortical responses to sensory stimuli (26–28). Because we developed a conceptual model and did not include many observed details of the barrel cortex, such as diversity of neuron types, the density of synaptic connections, etc., the model parameters may not be close the observed experimental values. We wanted to keep the model as simple as possible to make qualitative predictions of the cortex's behavior; we did not aim to make detailed quantitative predictions.

Network Architecture. To activate such a large population of layer 2/3 neurons, layer 4 neurons may diffusely project to layer 2/3. However, studies of layer 4 to layer 2/3 connectivity indicate that L4 axons project to the area in L2/3 just above the corresponding L4 barreloid (48). This suggests that whisker stimulations activate, via canonical thalamus → L4 → L2/3 excitatory circuits, a small population of L2/3 neurons located above the corresponding L4 column, and thus, population neural activity in L2/3 that spreads to many cortical columns must be evoked by horizontal connections. In the model, a small population of L2/3 neurons is located at the center of the network. These L2/3 neurons in turn activate other L2/3 neurons via horizontal connections, and the evoked activity propagates horizontally within L2/3 from the site of the initial activation. We did not model L4 neurons explicitly and instead injected currents directly into L2/3 neurons.

The model consisted of 10,000 excitatory and 2,500 inhibitory neurons, which were arranged in a 2D network, 100 by 100 neurons for the excitatory neurons and 50 by 50 for the inhibitory neurons.

The short-range connections were randomly assigned from a distance-dependent distribution (see *SI Materials and Methods* for more details). This procedure resulted in neighboring neurons having higher chances to be connected than distant neurons. The recurrent excitatory–excitatory connections were in the range observed among adjacent pyramidal neurons in L2/3 layer (26–28) and were randomly assigned for each pair of neurons with probability of 0.1. Recurrent connections between excitatory and inhibitory neurons were randomly connected with the peak probability 0.5.

The sparseness of the stimulus-evoked activity in L2/3 was critical to explain the observed neural response properties in L2/3. It was possible to observe traveling waves in a network consisting solely of the weak recurrent connections. However, the activation pattern in such network would not be sparse: the traveling waves would activate almost all neurons at the wavefront. In the model, the activated patterns were spatially sparse only when we added a few strong connections. In the model, out of 10,000 excitatory L2/3 neurons we randomly selected 1,000 neurons. Out of these 1,000 neurons, we randomly selected pairs of neurons and connected them with stronger synapses. We repeated this process until we reached the percolation threshold ~500 strong connections.

Neuron Model. The excitatory neurons were modeled after pyramidal neurons (29). The inhibitory neurons were modeled after fast-spiking PV interneurons (30) and provided both feedforward and recurrent inhibition into L2/3 excitatory neurons (49).

Both the excitatory and inhibitory neurons were simulated using integrate and fire neuron model (50) with different sets of parameters. When voltage of a neuron reached a threshold, the voltage was assigned a reset value −5. This value was selected to implicitly introduce refractory period; thus, it took a few milliseconds for a neuron to recover after spiking. The threshold for

each excitatory neuron was randomly selected from uniform distribution in a range from 0.5 to 2. Initial values for voltages were also randomly selected from a uniform distribution between 0 and 1.

For the excitatory neurons, after a neuron spiked, its voltage was changed to a reset value −5. This reset value was selected to implicitly introduce a refractory period; in the simulations, it took a few milliseconds for a neuron to recover after spiking. We did not model the refractory period in the inhibitory neurons.

Stimuli. In the model, we did not include the input layer 4 into the model but applied input currents directly into L2/3 neurons. We briefly activated a subset of L2/3 neurons located in the center of the network, corresponding to one cortical column. The stimuli lasted 2 ms. The short stimulation was due to feedforward inhibition that is prominent in L4–L2/3 projections and suppresses later spikes (31, 32). The directly activated L2/3 neurons then activated other L2/3 neurons via horizontal connections within the L2/3 network.

We stimulated a small population of randomly selected neurons in the center of L2/3 network, which mimicked inputs from layer 4 neurons. Stimuli were applied to randomly selected excitatory and inhibitory neurons in a square consisting of neurons 45 to 55 in both directions. The strengths of the input currents were randomly selected from a uniform distribution between 0 and 1.

ACKNOWLEDGMENTS. We thank David O'Keefe for useful discussions and help with manuscript preparation. This research was supported by the Howard Hughes Medical Institute, the NSF Temporal Dynamics of Learning Center (NSF Grants SBE 0542013 and SMA-1041755), the Office of Naval Research (N00014-15-1-2328), the Swartz Foundation, and the Kieckhefer Foundation.

1. Douglas RJ, Martin KA (2004) Neuronal circuits of the neocortex. *Annu Rev Neurosci* 27:419–451.
2. Hubel DH, Wiesel TN (1962) Receptive fields, binocular interaction and functional architecture in the cat's visual cortex. *J Physiol* 160:106–154.
3. Ohki K, Chung S, Ch'ng YH, Kara P, Reid RC (2005) Functional imaging with cellular resolution reveals precise micro-architecture in visual cortex. *Nature* 433:597–603.
4. Bonin V, Histed MH, Yurgenson S, Reid RC (2011) Local diversity and fine-scale organization of receptive fields in mouse visual cortex. *J Neurosci* 31:18506–18521.
5. Bandyopadhyay S, Shamma SA, Kanold PO (2010) Dichotomy of functional organization in the mouse auditory cortex. *Nat Neurosci* 13:361–368.
6. Sato TR, Gray NW, Mainen ZF, Svoboda K (2007) The functional microarchitecture of the mouse barrel cortex. *PLoS Biol* 5:e189.
7. Clancy KB, Schnepel P, Rao AT, Feldman DE (2015) Structure of a single whisker representation in layer 2 of mouse somatosensory cortex. *J Neurosci* 35:3946–3958.
8. Ferezou I, Bolea S, Petersen CC (2006) Visualizing the cortical representation of whisker touch: Voltage-sensitive dye imaging in freely moving mice. *Neuron* 50: 617–629.
9. Petersen CC (2007) The functional organization of the barrel cortex. *Neuron* 56: 339–355.
10. Kerr JND, et al. (2007) Spatial organization of neuronal population responses in layer 2/3 of rat barrel cortex. *J Neurosci* 27:13316–13328.
11. Margolis DJ, et al. (2012) Reorganization of cortical population activity imaged throughout long-term sensory deprivation. *Nat Neurosci* 15:1539–1546.
12. de Kock CP, Bruno RM, Spors H, Sakmann B (2007) Layer- and cell-type-specific suprathreshold stimulus representation in rat primary somatosensory cortex. *J Physiol* 581:139–154.
13. de Kock CP, Sakmann B (2009) Spiking in primary somatosensory cortex during natural whisking in awake head-restrained rats is cell-type specific. *Proc Natl Acad Sci USA* 106:16446–16450.
14. O'Connor DH, Peron SP, Huber D, Svoboda K (2010) Neural activity in barrel cortex underlying vibrissa-based object localization in mice. *Neuron* 67:1048–1061.
15. Hires SA, Gutnisky DA, Yu J, O'Connor DH, Svoboda K (2015) Low-noise encoding of active touch by layer 4 in the somatosensory cortex. *eLife* 4:e06619.
16. Brecht M, Roth A, Sakmann B (2003) Dynamic receptive fields of reconstructed pyramidal cells in layers 3 and 2 of rat somatosensory barrel cortex. *J Physiol* 553: 243–265.
17. Barth AL, Poulet JF (2012) Experimental evidence for sparse firing in the neocortex. *Trends Neurosci* 35:345–355.
18. O'Connor DH, et al. (2013) Neural coding during active somatosensation revealed using illusory touch. *Nat Neurosci* 16:958–965.
19. Buzsáki G, Mizuseki K (2014) The log-dynamic brain: How skewed distributions affect network operations. *Nat Rev Neurosci* 15:264–278.
20. Johnson BA, Frostig RD (2015) Long, intrinsic horizontal axons radiating through and beyond rat barrel cortex have spatial distributions similar to horizontal spreads of activity evoked by whisker stimulation. *Brain Struct Funct* 221:3617–3639.
21. Wester JC, Contreras D (2012) Columnar interactions determine horizontal propagation of recurrent network activity in neocortex. *J Neurosci* 32:5454–5471.
22. Sporns O (2011) *Networks of the Brain* (MIT Press, Cambridge, MA).
23. Yassin L, et al. (2010) An embedded subnetwork of highly active neurons in the neocortex. *Neuron* 68:1043–1050.
24. Benedetti BL, Takashima Y, Wen JA, Urban-Ciecko J, Barth AL (2013) Differential wiring of layer 2/3 neurons drives sparse and reliable firing during neocortical development. *Cereb Cortex* 23:2690–2699.
25. Song S, Sjöström PJ, Reigl M, Nelson S, Chklovskii DB (2005) Highly nonrandom features of synaptic connectivity in local cortical circuits. *PLoS Biol* 3:e68.
26. Feldmeyer D, Lübke J, Sakmann B (2006) Efficacy and connectivity of intracolumnar pairs of layer 2/3 pyramidal cells in the barrel cortex of juvenile rats. *J Physiol* 575: 583–602.
27. Lefort S, Tomm C, Floyd Sarria JC, Petersen CC (2009) The excitatory neuronal network of the C2 barrel column in mouse primary somatosensory cortex. *Neuron* 61:301–316.
28. Feldmeyer D, et al. (2013) Barrel cortex function. *Prog Neurobiol* 103:3–27.
29. Spruston N (2008) Pyramidal neurons: Dendritic structure and synaptic integration. *Nat Rev Neurosci* 9:206–221.
30. Markram H, et al. (2004) Interneurons of the neocortical inhibitory system. *Nat Rev Neurosci* 5:793–807.
31. Xue M, Atallah BV, Scanziani M (2014) Equalizing excitation-inhibition ratios across visual cortical neurons. *Nature* 511:596–600.
32. House DR, Elstrott J, Koh E, Chung J, Feldman DE (2011) Parallel regulation of feedforward inhibition and excitation during whisker map plasticity. *Neuron* 72: 819–831.
33. Erdős P, Rényi A (1960) On the evolution of random graphs. *Publ Math Inst Hung Acad Sci* 5:17–61.
34. Li L, Gainey MA, Goldbeck JE, Feldman DE (2014) Rapid homeostasis by disinhibition during whisker map plasticity. *Proc Natl Acad Sci USA* 111:1616–1621.
35. Crochet S, Poulet JF, Kremer Y, Petersen CC (2011) Synaptic mechanisms underlying sparse coding of active touch. *Neuron* 69:1160–1175.
36. Perrard S, Fort E, Couder Y (2016) Wave-based turing machine: Time reversal and information erasing. *Phys Rev Lett* 117:094502.
37. Yoshimura Y, Dantzker JLM, Callaway EM (2005) Excitatory cortical neurons form fine-scale functional networks. *Nature* 433:868–873.
38. Jouhanneau JS, et al. (2014) Cortical fosGFP expression reveals broad receptive field excitatory neurons targeted by POm. *Neuron* 84:1065–1078.
39. Watts DJ, Strogatz SH (1998) Collective dynamics of 'small-world' networks. *Nature* 393:440–442.
40. Hilgetag CC, Burns GA, O'Neill MA, Scannell JW, Young MP (2000) Anatomical connectivity defines the organization of clusters of cortical areas in the macaque monkey and the cat. *Philos Trans R Soc Lond B Biol Sci* 355:91–110.
41. Bassett DS, Bullmore E (2006) Small-world brain networks. *Neuroscientist* 12:512–523.
42. Gerhard S, et al. (2011) The connectome viewer toolkit: An open source framework to manage, analyze, and visualize connectomes. *Front Neuroinform* 5:3.
43. Gal E, et al. (2017) Rich cell-type-specific network topology in neocortical microcircuitry. *Nat Neurosci* 20:1004–1013.
44. Barabási A-L, Albert R (1999) Emergence of scaling in random networks. *Science* 286: 509–512.
45. Stauffer D, Aharony A (1994) *Introduction to Percolation Theory* (CRC Press, Boca Raton, FL).
46. Mandelbrot B (1982) *The Fractal Geometry of Nature* (Freeman and Company, New York).
47. Laughlin SB, Sejnowski TJ (2003) Communication in neuronal networks. *Science* 301: 1870–1874.
48. Feldmeyer D (2012) Excitatory neuronal connectivity in the barrel cortex. *Front Neuroanat* 6:24.
49. Isaacson JS, Scanziani M (2011) How inhibition shapes cortical activity. *Neuron* 72: 231–243.
50. Dayan P, Abbott LF (2001) *Theoretical Neuroscience* (MIT Press, Cambridge, MA).